Modelling the vegetation response to the 8.2 ka bp cooling event in Europe and Northern Africa

Huan Li, Hans Renssen, Didier M. Roche, Paul Miller

JOURNAL OF QUATERNARY SCIENCE (2019) **34**(8) 650–661 ISSN 0267-8179. DOI: 10.1002/jqs.3157

JQS Journal of Quaternary Science QRA Quaternary Research Association

Modelling the vegetation response to the 8.2 ka BP cooling event in Europe and Northern Africa

HUAN LI,[1]* HANS RENSSEN,[1,2] DIDIER M. ROCHE[1,3] and PAUL A. MILLER[4,5]

[1]Vrije Universiteit Amsterdam, Faculty of Sciences, Cluster Earth and Climate, De Boelelaan, 1085, Amsterdam, The Netherlands
[2]Department of Natural Sciences and Environmental Health, University of South-Eastern Norway, Gullbringvegen 36, N-3800, Bø i Telemark, Norway
[3]Laboratoire des Sciences du Climat et de l'Environnement, LSCE/IPSL, CEA-INSU-UVSQ-CNRS, Université Paris-Saclay, Gif-sur-Yvette, France
[4]Department of Physical Geography and Ecosystem Science, Lund University, Lund, Sweden
[5]Centre for Environmental and Climate Research, Lund University, Lund, Sweden

Received 20 December 2018; Revised 30 September 2019; Accepted 13 October 2019

ABSTRACT: The 8.2 ka BP cooling event is assumed to be the most clearly marked abrupt climate event in the Holocene at northern mid- to high latitudes. In this study, we simulate the vegetation responses to the 8.2 ka BP climate change event over Europe and Northern Africa. Our results show that all dominant plant functional types (PFTs) over Europe and North Africa respond to these climate changes, but the magnitude, timing and impact factor of their responses are different. Compared with pollen-based vegetation reconstructions, our simulation generally captures the main features of vegetation responses to the 8.2 ka BP event. Interestingly, in Western Europe, the simulated vegetation after perturbation is different from its initial state, which is consistent with two high-resolution pollen records. This different vegetation composition indicates the long-lasting impact of abrupt climate change on vegetation through eco-physiological and ecosystem demographic processes, such as plant competition. Moreover, our simulations suggest a latitudinal gradient in the magnitude of the event, with more pronounced vegetation responses to the severe cooling in the north and weaker responses to less severe cooling in the south. This effect is not seen in pollen records. © 2019 The Authors. Journal of Quaternary Science Published by John Wiley & Sons, Ltd.

KEYWORDS: 8.2 ka bp cooling event; long-lasting effects of abrupt climate change; LPJ-GUESS; plant functional types (PFTs); pollen reconstructions; vegetation simulations comparisons

Introduction

The worldwide distribution and character of vegetation depend mainly on climate conditions, and plants are likely to respond within decades when the amplitudes of climatic changes exceed the tolerance of the species, due to high mortality by frost, drought or other fatal damage to plant physiology (Tinner and Lotter, 2001). Moreover, vegetation can also be impacted by many other factors, including changed interspecific competition, forest fire and human disturbance. These vegetation responses caused by both climatic and ecological impacts are often described as 'regime shifts', referring to ecosystem reconfiguration between alternative stable states (Lees *et al.*, 2006; Andersen *et al.*, 2009). Understanding the mechanisms behind such rapid ecological responses is very important in the context of future climate change. One approach to improve this knowledge is to study the impact of past abrupt climate change on vegetation.

One prominent example of past climate change is the 8.2 ka BP cooling event that has been confirmed to be the highest magnitude abrupt climate event in the Holocene at northern mid- to high latitudes (Alley and Agustsdottir, 2005; Daley *et al.*, 2011). Both modelling and proxy-based studies suggest that the 8.2 ka BP event is the result of a weakened Atlantic meridional overturning circulation (AMOC) after a sudden injection of freshwater to the Labrador Sea from the Laurentide Ice Sheet and proglacial Lake Agassiz–Ojibway (Clarke *et al.*, 2004; Alley and Agustsdottir, 2005; Rohling and Pälike, 2005; Wiersma and Renssen, 2006; Daley *et al.*, 2011; Wagner *et al.*, 2013; Morrill *et al.*, 2014; Matero *et al.*, 2017). This event was characterized by a reduction in annual temperature in the Northern Hemisphere and an increase in seasonality, with stronger cooling in the boreal winter (by up to 30 °C) than summer (by up to 7 °C) at high latitudes (Wiersma and Renssen, 2006). It is marked by a 3.3 ± 1.1 °C transient cooling over ~160 years in Greenland (Kobashi *et al.*, 2007; Thomas *et al.*, 2007), declines of mean annual temperature between −0.6 and −1.2 °C around the circum-North Atlantic for 100–150 years and drier conditions over the Mediterranean and the Northern Hemisphere tropics (Morrill *et al.*, 2013). While such climate responses during the 8.2 ka BP event have been analysed in many previous studies, the spatio-temporal impacts of this climate change on vegetation remains relatively poorly known.

Simulations with dynamic global vegetation models (DGVMs) enable us to analyse the impacts of past climate events, and to evaluate the effects of separate climate factors (e.g. temperature or precipitation). However, only a very limited number of modelling studies have addressed the issue of the vegetation response to abrupt climate changes (Scholze *et al.*, 2003; Köhler *et al.*, 2005; Menviel *et al.*, 2008; Miller *et al.*, 2008; Bozbiyik *et al.*, 2011; Woillez *et al.*, 2013). For instance, Miller *et al.* (2008) simulated vegetation responses to an abrupt temperature increase 9 ka BP ago in Fennoscandia using LPJ-GUESS and compared their results to pollen

*Correspondence Huan Li, as above.
Email: h.li@vu.nl

accumulation rate data. Their study suggested that millennial variations in summer and winter temperatures determine vegetation dynamics and that biotic factors play key roles for plant species when near their bioclimatic limits. There are also several studies on vegetation responses to abrupt cooling. For example, Scholze *et al.* (2003) investigated vegetation changes during the Younger Dryas using the LPJ DGVM. Their results show that the strong cooling during the Younger Dryas leads to a decrease in temperate forests. The temperate forests were replaced by boreal forests and C3 grass in northwest Europe and by C3 grass only in Southern Europe. In addition, Woillez *et al.* (2013) used Last Glacial Maximum (LGM) climatic anomalies to force the ORCHIDEE DGVM. They investigated an important regression of forests and expansion of grasses in Europe during the LGM, driven by small decreases in mean temperature (about −1 to −2 °C) and precipitation (about −10 to −30%). In their case, the glacial vegetation was very sensitive to climatic variability because the initial climates were already very close to climatic thresholds of vegetation, highlighting the importance of the initial climate states for vegetation responses. Moreover, several studies have investigated the terrestrial carbon cycle during the LGM using DGVMs (Köhler *et al.*, 2005; Menviel *et al.*, 2008; Bozbiyik *et al.*, 2011). For instance, Köhler *et al.* (2005) found a southward shift of the tree line and a reduction of temperate and boreal forests in the Northern Hemisphere, but do not give more details on the spatio-temporal responses of vegetation distribution. Their results were in qualitative agreement with Menviel *et al.* (2008) and Scholze *et al.* (2003). In contrast, Bozbiyik *et al.* (2011) found strong reductions of carbon stocks in some tropical locations and in high northern latitudes, but they applied fixed pre-industrial vegetation in their climate simulations. However, the sensitivity of vegetation to abrupt climate change under interglacial climates remains unclear.

In this paper, we simulate vegetation responses to the 8.2 ka BP event as an example to examine the interglacial vegetation responses to abrupt climate change, using the LPJ-GUESS DGVM, in combination with the iLOVECLIM climate model. We take a two-step approach: we first simulate climate anomalies during the 8.2 ka BP event with the iLOVECLIM climate model, and subsequently we force LPJ-GUESS with these climatic anomalies to study the vegetation responses. We focus on vegetation responses over Europe and Northern Africa, where vegetation can be expected to have experienced relatively strong changes. Europe is also of particular interest given the pollen records available for a model–data comparison. The following questions will be addressed:

1. What is the spatial–temporal vegetation response to the 8.2 ka BP event? Where can we find significant changes in vegetation and to what extent is the vegetation response synchronous with climate change?
2. What is the relative contribution of temperature and precipitation anomalies to the vegetation response?
3. To what extent are vegetation simulations consistent with pollen-based reconstructions for the 8.2 ka BP event?

Material and methods

Model descriptions

The LPJ-GUESS vegetation model

LPJ-GUESS (Smith *et al.*, 2001, 2014) is a second-generation DGVM with explicit scaling of individual-level processes among several patches whose size is decided by the maximum area of influence of one full-grown individual plant on its neighbours (15 patches in this study) in each grid cell. The model version used in this study has representations of soil and plan nitrogen (N) dynamics described by Smith *et al.* (2014). Nitrogen deposition was kept constant at a pre-industrial level of 1 kgN ha^{-1} a^{-1} in our experiments. In this model, the parameterizations of biophysical and physiological processes (stomatal conductance and photosynthesis) are identical to the equilibrium model BIOME3 (Haxeltine and Prentice, 1996; Sitch *et al.*, 2003), although photosynthesis is reduced in the event that N supply cannot meet demand (Smith *et al.*, 2014). LPJ-GUESS simulates the distribution of 11 plant functional types (PFTs) and bare soil, because of transient climatic forcing and competition among different PFTs for light and water resources. It includes dynamic, stochastic representations of establishment, mortality, generic and fire disturbance, whereas growth, carbon allocation, plant allometry, phenology and turnover follow LPJ-DGVM. In this study, the model is forced 'offline' by monthly climatic inputs (temperature, precipitation and cloud cover) at T21 resolution from the iLOVECLIM model, implying no feedbacks between vegetation and climate are included.

Description of the climate model

iLOVECLIM is an updated version of LOVECLIM 1.2 (Goosse *et al.*, 2010; Roche *et al.*, 2014), and contains modules for the main climatic system components. Here we apply a version including the atmosphere (ECBilt), the ocean (CLIO) and terrestrial vegetation (VECODE). ECBilt is the atmospheric component, consisting of a three-level, quasi-geostrophic model at T21 resolution (Opsteegh *et al.*, 1998). The sea ice–ocean part (CLIO) consists of a three-dimensional, free surface ocean general circulation model coupled to a dynamic-thermodynamic sea-ice model (Goosse *et al.*, 2010). The horizontal resolution of CLIO is 3° latitude by 3° longitude, and there are 20 unevenly spaced vertical layers in the ocean. VECODE calculates vegetation cover in terms of two PFTs (grasses and trees) and bare soil as a dummy type at T21 resolution (Brovkin *et al.*, 1997). This vegetation cover is forced by climatic inputs from ECBilt, and in turn, VECODE calculates land surface albedo and passes it back to ECBilt.

By activating VECODE in iLOVECLIM, we already include in a crude way the impact of vegetation changes in our climate simulations. However, note that our goal for the iLOVECLIM simulations was to obtain 8.2 ka BP climate anomalies that are as close as possible to proxy-based evidence, to be used as forcing for LPJ-GUESS, so that we could evaluate the impact of this abrupt climate change on vegetation in considerable detail. We thus only consider the climatic output of iLOVECLIM, and do not evaluate the results of VECODE in this study. Because cloud cover is prescribed in iLOVECLIM, the transient climatic forcing of LPJ-GUESS consists only of varying temperature and precipitation.

Experimental design

The climate simulations

As the first step, we performed two different climatic simulations following Wiersma and Renssen (2006): a control simulation of the early Holocene (at 8.5 ka BP) equilibrium climate before the event and a simulation of the 8.2 ka BP event. The control simulation (8.5ka_CTRL) was run for 1000 years. It is a continuation of the 8.5 ka BP simulation (OGIS_FWF-v2) of Zhang *et al.* (2016) and the boundary conditions are identical with their 8.5 ka BP simulation. Atmospheric greenhouse gas concentrations were derived from ice core measurements (Loulergue *et al.*, 2008; Schilt

et al., 2010): $CO_2 = 260.35$ p.p.m., $CH_4 = 660.27$ p.p.b. and $N_2O = 260.58$ p.p.b.. We prescribed astronomical parameters from Berger (1978) (eccentricity = 0.019199, obliquity = 24.22168°, longitude of perihelion = 319.4947°), resulting in more insolation in the Northern Hemisphere during the boreal summer and less insolation during boreal autumn and winter compared to the present day. For example, the maximum and minimum monthly insolation anomalies at 60°N are 37 W m^{-2} (+8%) in June and −25 W m^{-2} (−18%) in October. The remnant Laurentide Ice Sheet (LIS) located around Hudson Bay was taken from ICE-5G (Peltier, 2004). Following Zhang *et al.* (2016), the baseline meltwater release for 1000 years in our control simulation includes 0.05 Sv of freshwater released at the St Lawrence River and 0.03 Sv at Hudson Strait and Hudson River, all from the LIS, and 0.022 Sv from the Greenland Ice Sheet (GIS).

In the 8.2 ka BP simulations (8.2ka_EVENT), we imposed an additional freshwater flux of 2.1 Sv (1 Sv = 10^6 m^3 s^{-1}) for 10 years (volume of 7.34×10^{14} m^3) in the Labrador Sea (50–65°N, 35–70°W), during which the background meltwater fluxes were kept at the same amount as in 8.5ka_CTRL (Table 1). To have a more realistic 8.2 ka BP climatic response, we tested different volumes of freshwater input, in which the simulation with 2.1 Sv freshwater for 10 years produced climate anomalies closest to this cold event. This freshwater volume (7.34×10^{14} m^3) is higher than the maximum constraint on the drained lake volume (1.63×10^{14} m^3) derived from the maximum sea-level rise following lake drainage (Törnqvist *et al.*, 2004), but lower than the ice saddle collapse volume (8.83×10^{14} m^3) inferred by Matero *et al.* (2017). After these 10 years, the simulation is continued for another 600 years with only background meltwater fluxes, which were reduced to 0.01 Sv for both the St Lawrence River and Hudson Strait, and 0.022 Sv for the GIS (Table 1; Zhang *et al.*, 2016). During the 8.2 ka BP event, large amounts of freshwater were injected into the Labrador Sea, and there is a rerouting of the continental runoff following the lake flood (Meissner and Clark, 2006). As a result, the amount of baseline freshwater decreases after the 8.2 ka BP event, and we keep these volumes of meltwater consistent with Zhang *et al.* (2016). Except for these freshwater fluxes, other forcings were identical to 8.5ka_CTRL. The total duration of the 8.2ka_EVENT simulation is thus 610 years.

The vegetation simulations

At the second step, we force LPJ-GUESS with the simulated climatic anomalies to study the vegetation responses (Table 2):

8.5ka_CTRL-LPJ: this is the 8.5 ka BP vegetation control simulation forced with a fixed 8.5 ka BP monthly mean climatology for 610 years. This climatology consists of monthly mean values, averaged over the last 200 years of the simulation 8.5ka_CTRL. The simulation started after a 2000-year spin-up phase starting from bare soil and forced with the identical fixed 200-year monthly climatology. The duration of 2000 years spin-up is long enough to reach an equilibrium vegetation state (Smith *et al.*, 2001). This 8.5ka_CTRL-LPJ experiment thus gives information about the vegetation dynamics in response to the 8.5 ka BP equilibrium climate.

Table 2. Vegetation simulations defined by names and forcings.

Experimental name	Initial conditions	Climate forcing
8.5ka_CTRL-LPJ	Bare soil	8.5ka_CTRL
8.2ka_EVENT-LPJ	8.5ka_CTRL-LPJ	8.2ka_EVENT
8.2ka_EVENT-LPJ-ts	8.5ka_CTRL-LPJ	ts from 8.2ka_EVENT, others from 8.5ka_CTRL
8.2ka_EVENT-LPJ-pp	8.5ka_CTRL-LPJ	pp from 8.2ka_EVENT, others from 8.5ka_CTRL

8.2ka_EVENT-LPJ: this 8.2 ka BP vegetation simulation starts from the end of 8.5ka_CTRL-LPJ and is forced for 580 years with annually varying climate forcing from simulation 8.2ka_EVENT. The 580 years of climate forcing are monthly climate values from the 31st to the 610th year of 8.2ka_EVENT (Fig. 1). As seen in Fig. 1, the first 30 years of the 8.2ka_EVENT climate simulation are characterized by a cold–warm oscillation, followed by a clear cooling response starting at year 31. To facilitate interpretation of the 8.2 ka BP vegetation response, we did not apply this cold–warm oscillation as forcing for LPJ-GUESS.

Two additional simulations, starting from the end of 8.5ka_CTRL-LPJ, are performed to test the relative impact of temperature and precipitation changes on vegetation during the 8.2 ka BP event:

8.2ka_EVENT-LPJ-ts (580 years): identical fixed climatic forcings as for 8.5ka_CTRL-LPJ except for the temperature, which is identical with transient forcing for 8.2ka_EVENT-LPJ.

8.2ka_EVENT-LPJ-pp (580 years): identical fixed climatic forcings as for 8.5ka_CTRL-LPJ except for the precipitation, which is identical with transient forcing for 8.2ka_EVENT-LPJ.

To characterize robust vegetation responses, we separate Europe into five sub-regions according to their geographical locations (Fig. 2). In each sub-region, we apply a moving two-tailed *z*-test (Chervin and Schenider, 1976) to the evolution of the main PFTs whose cover is larger than 5% (except 'Tropical trees' in Southern Europe) to discuss these regional characteristic PFT distributions. This *z*-test assesses whether the vegetation is statistically different from the initial state (the initial state here is the 8.5 ka BP vegetation equilibrium state). To detect a vegetation signal of several decades, we classify a data point in our simulated vegetation time series as anomalous if the average of the moving window is different from the equilibrium state with 99% certainty. Similar to Wiersma *et al.* (2011), we use 31-year centred moving windows (t − 15 a, t + 15 a) from simulation 8.2ka_EVENT-LPJ. The equilibrium state is taken from simulation 8.5ka_CTRL-LPJ, which consists of a more than 200-year-long equilibrium run. As a result, the equilibrium state is calculated

Table 1. Climatic simulations defined by names and forcings.

Experimental name	Initial conditions	Freshwater forcing (FWF)
8.5ka_CTRL	8.5 ka BP climate from Zhang et al. (2016)	**Background FWF_1** (*1) for 1000 years
8.2ka_EVENT	**8.5ka_CTRL**	**Perturbation FWF** (*2) + **Background FWF_1** (*1) for 10 years; **Background FWF_2** (*3) for 600 years;

*1: background freshwater_1: 0.05 Sv (St Lawrence River) + 0.03 Sv (Hudson Strait) + 0.022 Sv (GIS).
*2: perturbation freshwater: 2.1 Sv (Labrador Sea; 50–65 N, 35–70 W).
*3: background freshwater_2: 0.01 Sv (St Lawrence River) + 0.01 Sv (Hudson Strait) + 0.022 Sv (GIS)

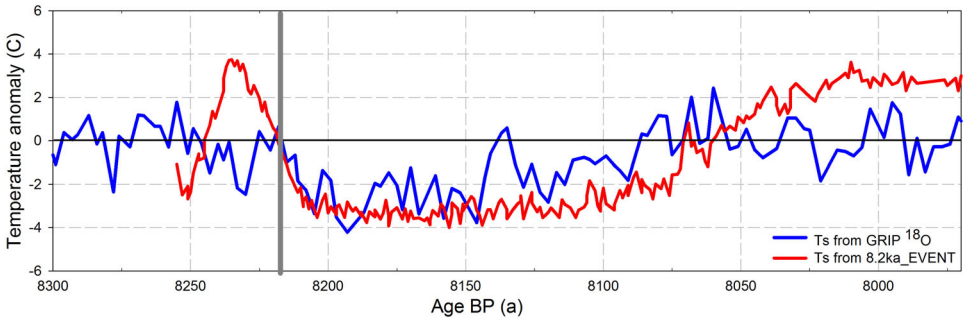

Figure 1. Time series of surface air temperature over central Greenland in 8.2ka_EVENT (red) compared to the GRIP temperature (blue) reconstruction from ice core $\delta^{18}O$ (Thomas et al., 2007). The vertical grey bar indicates the start of the 8.2 ka BP event climatic forcings input to LPJ-GUESS, which is the 31st year of the 8.2ka_EVENT simulation. [Color figure can be viewed at wileyonlinelibrary.com].

based on the last 200 years of simulation of 8.5ka_CTRL-LPJ. This *z*-test window moves along the time series with 1-year time step, comparing the variance and average of the moving window and the equilibrium state, producing a time series of *z*-values. We then detect robust vegetation responses and durations according to significant *z*-values at the 99% confidence level. Moreover, we assess the individual contributions of temperature and precipitation changes during the 8.2 ka BP event to these vegetation responses. These contributions ($C_{ts,pp}$) are expressed in percentages of PFT anomalies as follows:

$$C_{ts,pp} = \frac{VD_{8.2ka\_EVENT\text{-}LPJ_{ts,pp}} - VD_{8.2ka\_EVENT\text{-}LPJ}}{VD_{8.2ka\_EVENT\text{-}LPJ} - VD_{8.5ka\_EVENT\text{-}LPJ}}$$

where VD refers to the respective vegetation distribution. The contribution equals 100% when temperature or precipitation alone causes identical vegetation responses to the responses suggested in 8.2ka_EVENT-LPJ, and can extend by 100% due to synergy effects between temperature and precipitation conditions.

Results and discussion

We focus on simulated vegetation responses to the 8.2 ka BP cooling event in this section. The simulated 8.2 ka BP temperature signals agree with the anomalies as reconstructed by terrestrial records (Morrill *et al.*, 2013) (Supporting Information Figs S4 and S5), indicating a mean annual cooling of about 1.0°C over parts of Europe with this cooling predominantly reflecting winter (DJF) and spring (MAM) signals in Europe (Fig. S6). Similar to previous studies (Wiersma and Renssen, 2006; Matero *et al.*, 2017), our simulations suggest relative dryness in most regions of Europe and North Africa during the 8.2 ka BP event but do not reproduce the increased precipitation in northern Europe indicated by geological records from Sweden and Norway (Morrill *et al.*, 2013). The simulated climate conditions are presented in the Supporting Information.

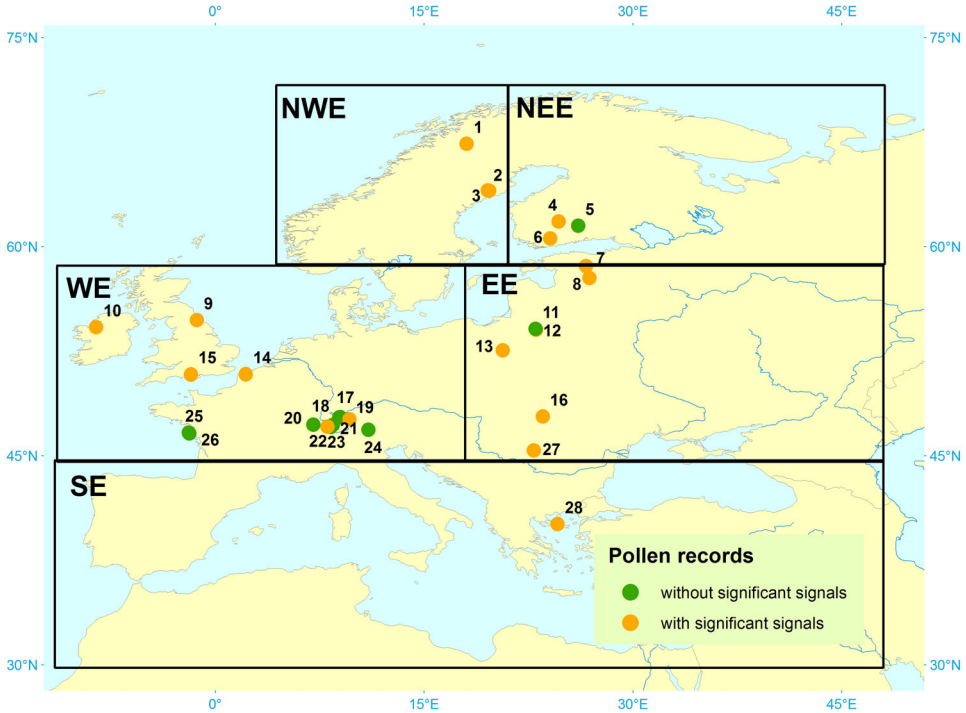

Figure 2. Sub-regions for investigating the vegetation responses to the 8.2 ka BP event. NWE, North-Western Europe; NEE, North-Eastern Europe, WE, Western Europe; EE, Eastern Europe; SE, Southern Europe; NA, Northern Africa. Numbers refer to the sites with high-resolution pollen records used in the text; the green and orange circles represent pollen records without and with significant 8.2 ka BP signals, respectively. Detailed information about these pollen records is given in Table S1. [Color figure can be viewed at wileyonlinelibrary.com].

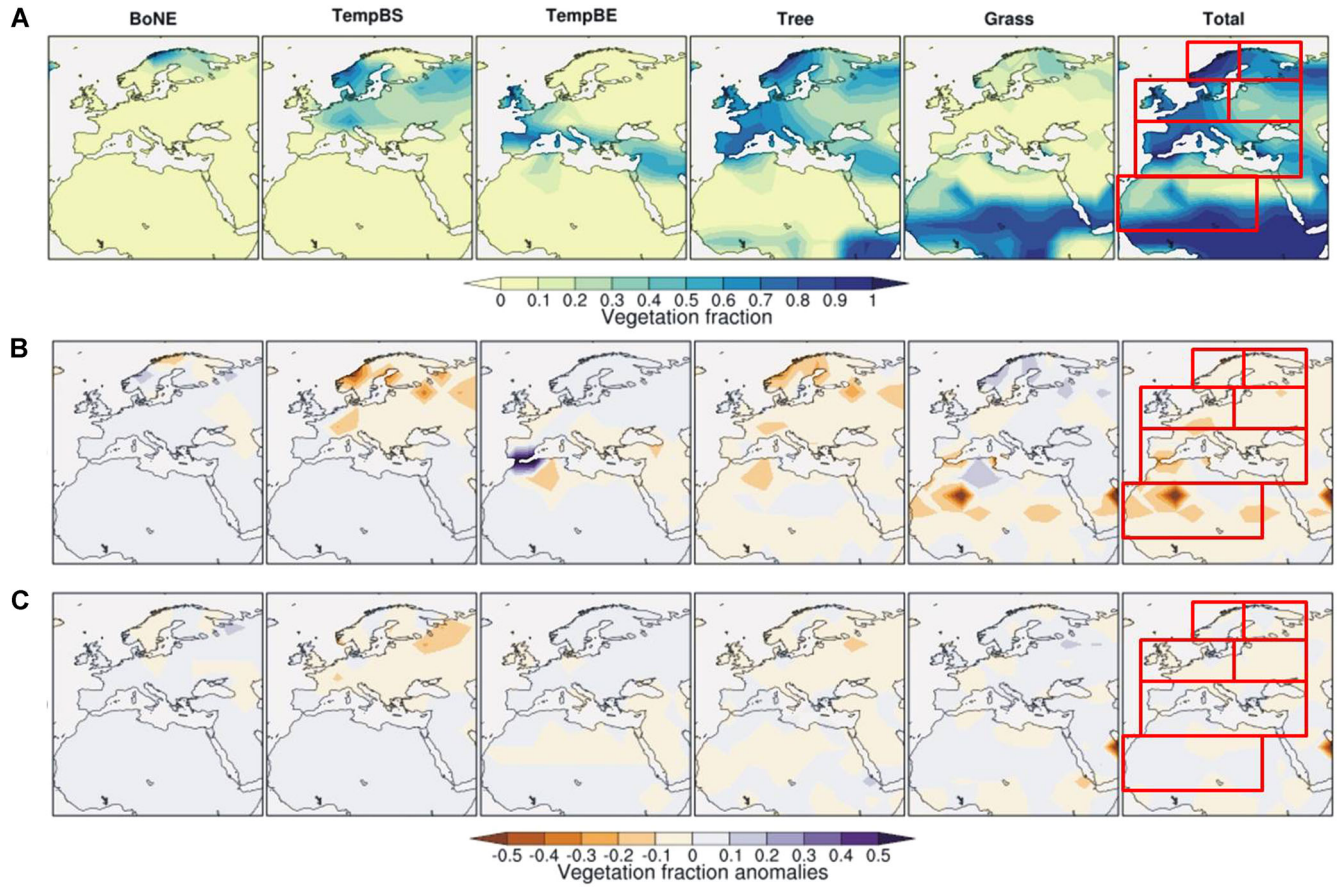

Figure 3. Simulated vegetation distributions under climatic forcing simulated by (A) 8.5 ka BP early Holocene climate, (B) during the 8.2 ka BP event and (C) after the perturbation of the 8.2 ka BP event. The values for A are means over the last 200 years of the runs 8.5ka_CTRL-LPJ. The values for B are vegetation responses, shown as anomalies of means over the strongest 50 years (from 91 to 140 years of the runs 8.2ka_EVENT-LPJ) during the run 8.2ka_EVENT-LPJ from A. The values for C are anomalies of means over the last 200 years of the runs 8.2ka_EVENT-LPJ from A. Simulated vegetation distributions are represented by main PFTs in this region. BoNE, boreal needle-evergreen trees; TempBS, temperate broadleaved summergreen trees; TempBE, temperate broadleaved evergreen trees. 'Tree' represents the sum fraction of tree PFTs, and 'grass' is the sum fraction of grass PFTs. 'Total' indicates the sum fraction of all PFTs. [Color figure can be viewed at wileyonlinelibrary.com].

Vegetation in the control run (8.5ka_CTRL-LPJ)

The overall 8.5 ka vegetation in Europe is dominated by high tree cover, with regional differences in PFT fractions (Fig. 3A). North-Western Europe (NWE) and North-Eastern Europe (NEE) have the same dominant PFTs but in different proportions. NWE has 49% temperate broadleaved summergreen trees (TempBS) and 18% Boreal needle evergreen trees (BoNE, Fig. 4a), while NEE has 32% TempBS and 13% BoNE (Fig. 4b). Grass covers about 20% in both regions, with slightly higher fractions in NEE than in NWE. In contrast, Western Europe (WE) has much higher proportions of temperate trees, with 20% temperate broadleaved evergreen trees (TempBE) and 37% TempBS (Fig. 4c). Tree cover in Eastern Europe (EE) is dominated by TempBS (31%, Fig. 4d). Southern Europe (SE) is dominated by TempBE (30%, Fig. 4e), mixed with a rather small fraction of tropical trees (2%) in its southern part. In these three regions, grass cover is about 10%. Different from vegetation in Europe, grass (37%) is the only dominant PFT in North Africa (Fig. 4f), combined with rare occurrences of TempBE and Tropical trees (both <2%).

Vegetation responses to the 8.2 ka BP event

All dominant PFTs respond to the 8.2 ka BP event, but the temporal response is not equal for each PFT (Fig. 4). In all regions, TempBS and grass react at the beginning of the cooling, while TempBE lags behind TempBS by 20–30 years in WE (Fig. 4c) and BoNE also lags behind TempBS by about 30 years in northern Europe (NWE and NEE, Fig. 4a,b).

In northern Europe, TempBS cover decreases at the beginning of the 8.2 ka BP cold event and reaches its minimum (32 and 18% in NWE and NEE, respectively), implying a reduction of about 17 and 14% in both regions in 50 years (Fig. 4a,b). TempBS disappears in the northern regions and dominates the southern part of these regions (Fig. 3B). At the same time, grasses expand over areas primarily occupied before by TempBS (Fig. 3B), with a maximum cover of 22%. By contrast, BoNE cover increases slightly after the 8.2 ka BP cooling event, yet it experiences a significant expansion after the minimum of TempBS and reaches its maximum [20 and 12% in NWE and NEE, respectively, representing increases of 12% (NWE) and 5% (NEE)] in 100 years (Fig. 4a,b). However, in the northern part of NWE, BoNE cover decreases where grass expands and it invades southward. Overall, our results thus indicate that the grass–BoNE and BoNE–TempBS boundaries move southward.

In mid-latitude Europe (WE and EE) the response time to the 8.2 ka BP event varies among different temperate tree PFTs. In WE (Fig. 4c), TempBS reaches its minimum (30%) in about 20 years, but TempBE responds to the 8.2 ka BP event more slowly than TempBS, reaching its minimum (18%) in around 60 years. In EE (Fig. 4d), TempBS decreases also at the beginning of the 8.2 ka BP event, and is reduced by 5%. However, grass cover does not expand as in Northern Europe,

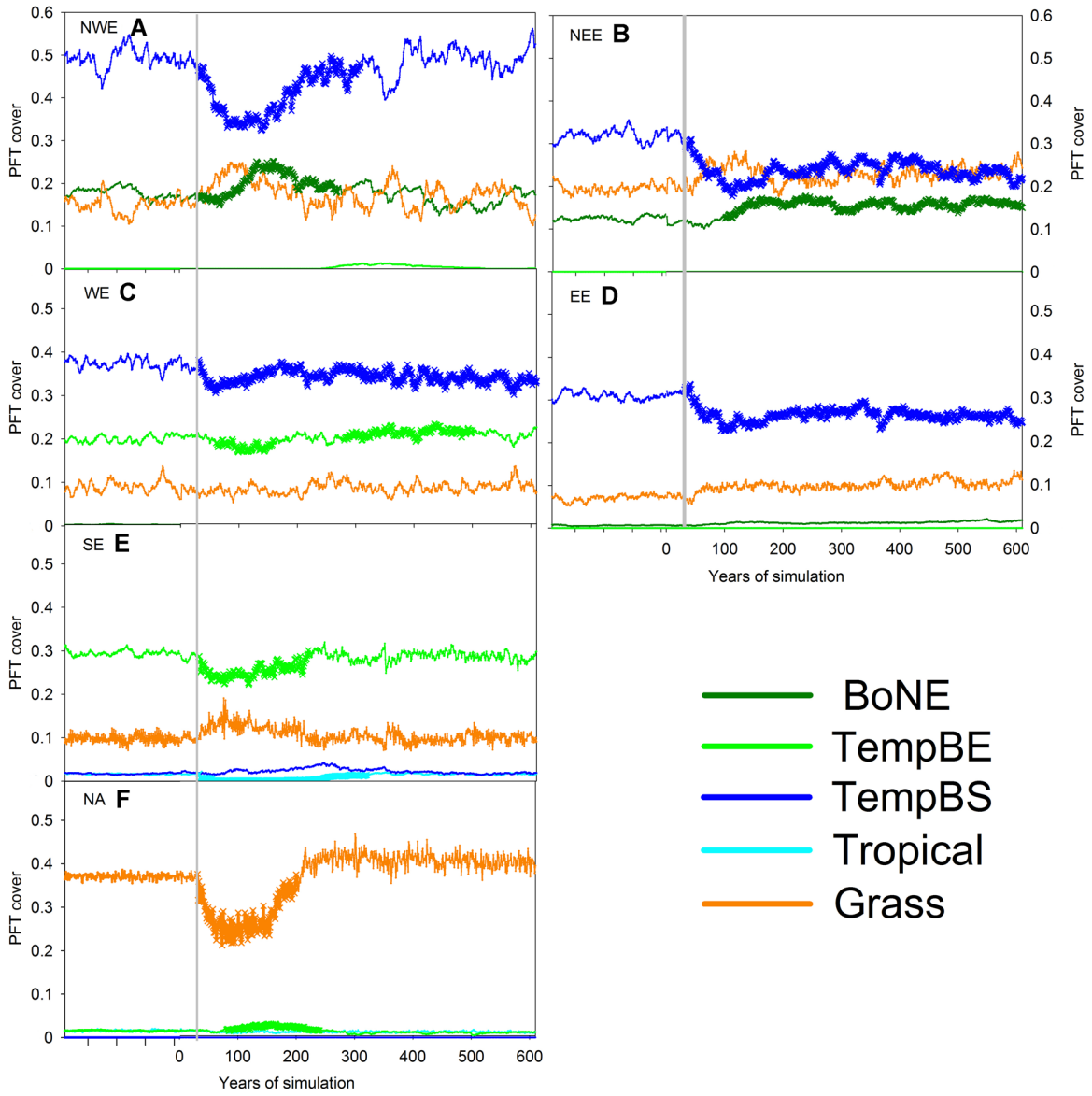

Figure 4. Temporal evolution of main PFT cover over (a) North-Western Europe (NEE),(b) North-Eastern Europe (NEE), (c) Western Europe (WE), (d) Eastern Europe (EE), (e) Southern Europe (SE) and (f) Northern Africa (NA) in 8.5ka_CTRL-LPJ and 8.2ka_EVENT-LPJ. The vertical grey bar indicates the start of the climatic 8.2 ka BP event perturbation. Bold lines indicate the statistically significant (99% level) vegetation responses during the 8.2 ka BP event, based on a two-tailed *z*-test (Wiersma et al., 2011), with 8.5ka_CTRL-LPJ as reference. [Color figure can be viewed at wileyonlinelibrary.com].

leading to a stronger reduction of total vegetation cover in WE and EE.

In southern regions, the vegetation responses to the 8.2 ka BP event in Southern Europe (SE) are very different from North Africa (NA). In SE, TempBE and grasses experience slight changes during the 8.2 ka BP event, but tropical trees disappear when the cooling starts (Fig. 4e). In contrast, in NA grasses decrease at the beginning of the 8.2 ka BP cold event from 37% to about 22% in 50 years, after which a rather slight expansion of TempBE (Fig. 4f) is simulated.

After the 8.2 ka BP event, most PFT fractions recover to their initial (8.5 ka BP) levels (Fig. 3C) in about 200 years, except for TempBS. In NEE, WE and EE, TempBS remains at a relatively stable level with only a modest recovery (Fig. 4b–d). This suggests that the 8.5 ka BP climate condition is very close to TempBS climatic thresholds and TempBS is therefore very sensitive to climate variability, leading to the establishment of another stable vegetation composition after the 8.2 ka BP perturbation. This implies that other PFTs benefit from climate perturbation. Consequently, this vegetation response indicates that abrupt climate changes can potentially trigger a transition between different stable vegetation compositions.

Relative impact of changes in temperature and precipitation on vegetation cover

Our comparison of 8.2ka_EVENT_LPJ (full climatic forcing) with the experiments with temperature anomaly-only forcing (8.2ka_EVENT_LPJ-ts) or precipitation anomaly-only forcing (8.2ka_EVENT_LPJ-pp) reveals that the importance of these two climate factors is different for the various PFTs in each sub-region.

For both BoNE (Fig. 5a) and TempBS (Fig. 5b) in northern Europe, temperature is clearly the dominant factor. In this region, cooler conditions are simulated, with up to −1.8 °C mean annual temperature decrease in NWE and a decline of about 1.0 °C in NEE. This cooling produced a response in BoNE and TempBS that is very similar in both 8.2ka_EVENT-LPJ and 8.2ka_EVENT-LPJ-ts, showing that temperature is the main driver. This similarity is clear at the beginning and the coldest phase of the 8.2 ka BP event. During the coldest phase, the contributions of temperature anomalies (Fig. 6) to both BoNE and TempBS are more than 100% in NWE. In NEE, the lower temperature also contributes more than 50% to both BoNE and TempBS.

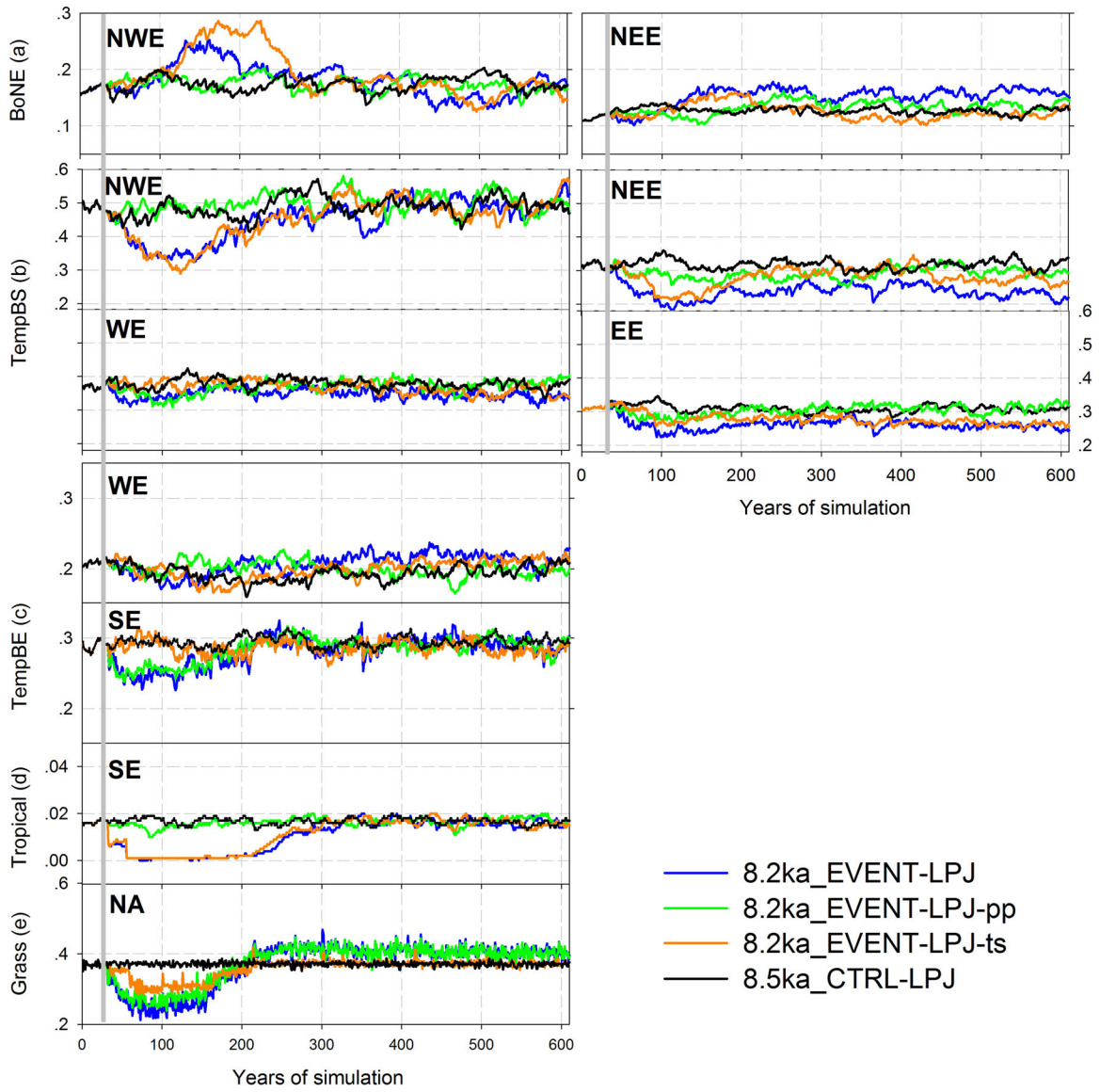

Figure 5. Fractions of main PFTs over Europe in 8.5ka_CTRL-LPJ (black), 8.2ka_EVENT-LPJ (blue), 8.2ka_EVENT-LPJ-pp (green) and 8.2ka_EVENT-LPJ-ts (orange). (a) BoNE over NWE and NEE; (b) TempBS over NWE, NEE, WE and EE; (c) TempBE over WE and SE; (d) Tropical trees over SE; and (e) Grass over NA. The vertical grey bar indicates the start of the climatic 8.2 ka BP event perturbation. NEE, North-Western Europe; NEE, North-Eastern Europe; WE, Western Europe, EE, Eastern Europe; SE Southern Europe; NA, Northern Africa. BoNE, Boreal needle evergreen trees; TempBS, temperate broadleaved summer-green trees; TempBE, temperate broadleaved evergreen trees. [Color figure can be viewed at wileyonlinelibrary.com].

The declines of TempBS (Fig. 5b) in WE and EE and TempBE (Fig. 5c) in WE are caused by changes in both temperature and precipitation. In these regions, the vegetation responses in 8.2ka_EVENT-LPJ show a clear decline, but the decline is weaker in both 8.2ka_EVENT-LPJ-ts and 8.2ka_EVENT-LPJ-pp. However, in EE, the sum of the latter two responses is more or less the same as the total response in 8.2ka_EVENT-LPJ, which is consistent with their up to 99% overlaid contributions (Fig. 6). In contrast, in WE, the synergy effects of temperature and precipitation anomalies contribute more than 50% to both

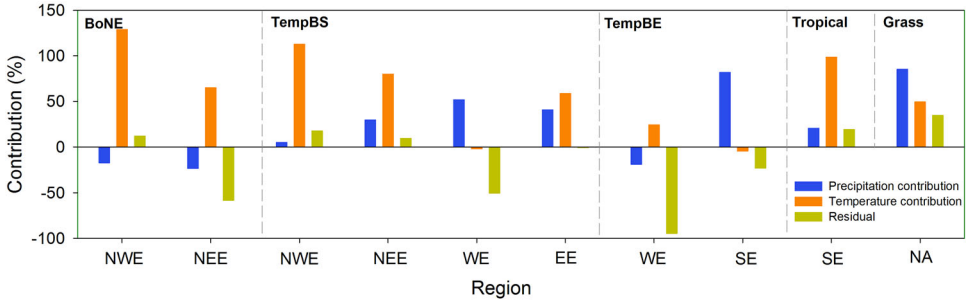

Figure 6. Contributions of temperature and precipitation to dominant PFTs in each sub-region. Blue and orange bars indicate contributions of precipitation and temperature, respectively; and dark yellow bars indicate contributions of their synergy effects. The contributions are calculated based on 50-year mean PFT anomalies of runs 8.2ka_EVENT-LPJ, 8.2ka_EVENT-LPJ-pp and 8.2ka_EVENT-LPJ-ts. The 50-year windows for each PFT are decided by their largest anomalies of runs 8.2ka_EVENT-LPJ compared to their 8.5 ka BP values. [Color figure can be viewed at wileyonlinelibrary.com].

TempBS and TempBE changes, implying the importance of lower temperature on weakening vegetation drought stress through reductions of evaporation.

TempBE (Fig. 5c) depends highly on precipitation in SE, while tropical trees (Fig. 5d) are more sensitive to temperature anomalies. In both 8.2ka_EVENT_LPJ and 8.2ka_EVENT_LPJ-pp, TempBE declines at a similar rate, reaching a cover of 25%, and implying a reduction of 5% compared to the control state. During the 50 years with lowest TempBE cover in 8.2ka_EVENT_LPJ, the contribution of precipitation anomaly reaches 82% (Fig. 6). In contrast, the cover of tropical trees (Fig. 5d) is very small, and tropical trees disappeared when the cooling starts in both 8.2ka_EVENT_LPJ and 8.2ka_EVENT_LPJ-ts. The contribution of temperature anomalies to tropical trees is up to 95% (Fig. 6).

As the only dominant PFT in NA, the decline of grass cover (Fig. 5e) is caused by changes in both temperature and precipitation, in which the > 50% decreases in summer precipitation dominate grass responses. The dominant role of precipitation to grass cover in NA has also been suggested by Lu *et al.* (2018). In this region, grass cover in 8.2ka_EVENT-LPJ shows a clear decline and this decline is stronger than in both 8.2ka_EVENT-LPJ-ts and 8.2ka_EVENT-LPJ-pp. However, the sum of the latter two responses is stronger than the total response in 8.2ka_EVENT-LPJ, indicating the counteractive effect of lower temperature and less precipitation on grass cover during the 8.2 ka BP event. This counteractive effect is also indicated by the 35% contributions of synergy effects (Fig. 6).

Model–data comparisons in specific regions

In this section, we will first compare directly simulated and reconstructed vegetation for the Early Holocene, followed by a discussion of the pollen-based evidence for vegetation change during the 8.2 ka BP event and a comparison with our model results. A large number of pollen records over Europe cover the time span of the 8.2 ka BP event, but not all of them have a sufficiently high time resolution and can be used to resolve vegetation changes associated with this event (Fig. 2). There are also high-resolution pollen records that do not indicate the 8.2 ka BP signals (green dots in Fig. 2), indicating either that the climate event was not as severe at that particular location, or that the vegetation response is too weak to show up in a pollen diagram. Some of these records are close to those that do show a clear response during the time of the 8.2 ka BP event (orange dots in Fig. 2), especially in the area around the Alps. This could suggest that the vegetation response to the 8.2 ka BP event depends on topographic differences that can be expected in such a mountainous region, affecting local conditions (altitude, aspect, slope, etc.) that impact climate and vegetation growth. Because the purpose of including pollen records in this study is to evaluate if our modelled vegetation responses are sensible and in line with actual vegetation responses, a further evaluation of these local effects and their influence on the detection of these climate impacts on vegetation in pollen records is outside the scope of this paper, so we have not discussed them further. Therefore, in this study, model evaluation is based on a selection of high-resolution pollen records that have been unambiguously used in previous studies that address the impact of the 8.2 ka BP climate anomaly on vegetation (Fig. 2).

Early Holocene vegetation

Our simulated distributions of the main PFTs generally agree with PFTs of the main pollen types during the early Holocene. The dominant distribution of BoNE in northern Scandinavia agrees with data indicating the development of boreal forest (Rosén *et al.*, 2001). Our simulation suggests that a mixture of temperate and boreal forest (TempBS and BoNE) persists in the southern part of NWE. This agrees with pollen-based reconstructions: for example, *Corylus*-dominated forest mixed with *Pinus*, *Betula*, *Alnus*, *Ulmus*, *Tilia* and *Quercus* at HøjbySø in Denmark (Hede *et al.*, 2010), and mixed forest with *Pinus, Betula* and *Alnus* in northern Sweden (Snowball *et al.*, 2002) and western Norway (Nesje *et al.*, 2006). However, we simulate a higher percentage of TempBS than BoNE in this region, whereas pollen records suggest a higher proportion of boreal tree species than temperate tree species. Besides model uncertainties, this discrepancy may be related to the over-representation of *Pinus* pollen due to its long-distance dispersal (Xu *et al.*, 2007). Over WE and EE, the early Holocene vegetation in our simulation is dominated by TempBS and TempBE, mixed with < 10% BoNE fraction. This vegetation distribution is consistent with pollen-based reconstructions at low altitudes, indicating mixed-temperate forest dominated by *Corylus*, *Ulmus*, *Tilia*, *Quercus*, etc. (Tinner and Lotter, 2001; Feurdean and Bennike, 2004; Veski *et al.*, 2004; Joly and Visset, 2009; Pál *et al.*, 2016), but the distribution of *Pinus* (BoNE) at upper elevations is not captured by our model due to the coarse resolution. In SE, TempBE (*Quercus*.evergreen in pollen records) becomes the dominant tree PFT (Kotthoff *et al.*, 2008) in both simulation and reconstructions.

Comparison of reconstructed and modelled vegetation responses

Our simulation (Fig. 4) generally captures the main features of vegetation responses recorded by palaeobotanical evidence (Table S1), indicated by comparable specific pollen taxa and evolutions of PFTs. However, there remain some discrepancies between pollen reconstructions and model simulations.

Northern Europe

The simulated declines of TempBS (Fig. 4a,b) are consistent with rapid declines of temperate, thermophilous broadleaved trees such as *Alnus, Corylus* and *Ulmus,* and expansions of BoNE (Fig. 4a,b) agree with increases in boreal trees such as *Pinus* (Seppä and Poska, 2004; Veski *et al.*, 2004; Head *et al.*, 2007; Sarmaja-Korjonen and Seppä, 2007; Ghilardi and O'Connell, 2013; Novenko and Olchev, 2015; Torbenson *et al.*, 2015; Fiłoc *et al.*, 2017; Hede *et al.*, 2010). According to Seppä *et al.* (2007), this decrease in temperate tree pollen percentages can be interpreted as a reflection of decreasing spring temperature. Our dominant factor analysis agrees with this interpretation. Moreover, the decline in *Betula* and expansion of grasses (for example Sjuodjijaure, site 1 in NWE; Rosén *et al.*, 2001) in the northern part of Northern Europe are also reflected in our simulations (Fig. 3). However, there are discrepancies between simulations and reconstructions. In the reconstructions, thermophilous deciduous tree pollen taxa often account for only a small proportion of the total, while the associated PFT (TempBS) is the dominant PFT in the model results. This discrepancy might be interpreted as reflecting over-representation of *Pinus* in the pollen-based reconstruction due to its long-distance dispersal (Xu *et al.*, 2007). Also, there are uncertainties related to simulated early Holocene climate and uncertainties associated with comparing pollen percentages with PFT cover (Miller *et al.*, 2008; Seppä *et al.*, 2009).

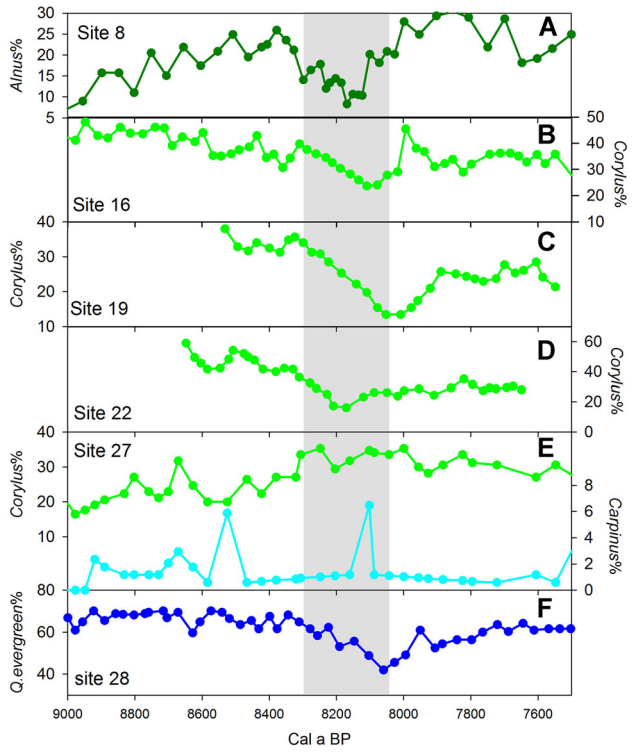

Figure 7. Selected pollen taxa percentage curves at 9000–7500 cal a BP from six sites in Europe. See Fig. 2 for the locations of the sites. (a) *Alnus* from site 8 (Veski et al., 2004); (b) *Corylus* from site 16 (Feurdean and Bennike, 2004); (c) *Corylus* from site 19 (Tinner and Lotter, 2001); (d) *Corylus* from site 22 (Tinner and Lotter, 2001); (e) *Corylus* and *Carpinus* from site 27 (Pál et al., 2016); and (f) *Quercus*.evergreen from site 28 (Kotthoff et al., 2008). The vertical grey shading indicates the signals of vegetation responses during the 8.2 ka BP event. [Color figure can be viewed at wileyonlinelibrary.com].

Mid-latitude Europe

During the 8.2 ka BP event, a reduction of temperate tree cover is indicated by the model and reconstructions (Tinner and Lotter, 2001; Seppä and Poska, 2004; Veski *et al.*, 2004; Feurdean *et al.*, 2008; Ghilardi and O'Connell, 2013; Novenko and Olchev, 2015; Pál *et al.*, 2016; Fiłoc *et al.*, 2017) and the impacts of changes in temperature and precipitation on vegetation vary in different regions. Rapid declines of temperate thermophilous broadleaved trees (*Alnus, Corylus*, etc.) in northern EE (site 8; Fig. 7a) are a result of cold winters and early springs because *Alnus* is strictly constrained by lower temperatures and a short growing season and is particularly sensitive to frost damage in early spring (Veski *et al.*, 2004). In southern EE (site 27 in EE; Fig. 7e), the percentage of *Corylus* shows comparable declines as in Estonia (site 8) but an expansion of *Carpinus* was found (Pál *et al.*, 2016). These vegetation responses attest to an increase in available moisture in winter and spring (Pál *et al.*, 2016) as this species has lower drought resistance than *Corylus* (Sykes *et al.*, 1996). In contrast, in middle EE (site 16), the large decline of *Corylus* has been interpreted as indicative of drier conditions (Fig. 7b; Feurdean and Bennike, 2004; Feurdean *et al.*, 2008). Moreover, in WE (sites 19 and 22; Fig. 7c,d), the decrease in TempBS (*Corylus*) and expansions of *Pinus*, *Betula*, *Tilia*, *Fagus* and *Abies* are interpreted as reflecting a cooling and reduced drought stress during the 8.2 ka BP event (Tinner and Lotter, 2001). Their interpretations of increases in available moisture during the growing season partially agree with Pál *et al.* (2016), but the vegetation responses in WE are stronger than those in EE (Pál *et al.*, 2016).

After the 8.2 ka BP event, TempBS cover (Fig. 4c) remains at a relative lower level compared to TempBS cover at 8.5 ka BP, indicating a persistent impact of this abrupt climate change. The two different compositions of PFT cover before and after the 8.2 ka BP event imply the possibility of different vegetation compositions under similar climate conditions. These different vegetation compositions reflected by our simulations are consistent with two high-resolution pollen-based reconstructions (sites 19 and 22). In the reconstructions by Tinner and Lotter (2001), the pollen percentage of *Corylus* does not recover to its early Holocene level after the 8.2 ka BP event (Fig. 7c,d). According to Tinner and Lotter (2001), the vegetation composition changed to include more drought-sensitive (*Tilia, Fagus, Abies*, etc.) and taller growing species (such as *Pinus*) due to the 8.2 ka BP climatic perturbation. Denser, more shaded stands formed during the cooling event, putting *Corylus* at a disadvantage as it is light-demanding and relatively short in stature, although the climatic conditions are more suitable for growth after the perturbation. Such competitive effects, in addition to composition changes resulting from changes in bioclimatic preferences, can be simulated in a realistic manner by LPJ-GUESS (Smith *et al.*, 2001; Seppä *et al.*, 2015). This implies that abrupt climate change could trigger vegetation changes among different stable vegetation compositions, which is supported by our simulation (Figs 4,5). In addition, our simulations suggest such long-lasting impacts of abrupt climate change in NEE and EE (Fig. 4b,d), but there is no pollen record tio allow detailed comparisons.

Southern Europe

There is an agreement between simulations and reconstructions (Davis and Stevenson, 2007; Kotthoff *et al.*, 2008) on a distinct decrease in TempBE (*Quercus*.evergreen in pollen) and an increase in grass (e.g. *Ephedra* in pollen), related to both lower temperature and drought stress. Up to 40% increases in herb and the persistent presence of *Ephedra* is seen as the result of increased drought stress (site 28 in SE; Kotthoff *et al.*, 2008). Moreover, the decline of *Quercus*.evergreen (Fig. 7f) is interpreted as being due to reduced winter precipitation and/or temperature (Davis and Stevenson, 2007). This is reflected in our dominant factor analysis (Fig. 5c).

Potential importance of initial climate and vegetation conditions

Our simulations suggest a weaker importance of initial states compared to experiments performed for the last glacial climate and vegetation. Woillez *et al.* (2013) studied vegetation responses to climate change during glacial periods and found shifts in dominant PFTs and a strong dependence on the initial state. In their experiments, the climate changes by about 1–2°C in Europe, similar to our 8.2 ka BP anomalies. Woillez *et al.* (2013) interpreted the clear glacial vegetation response as reflecting the climate being very close to the climatic threshold of the vegetation, leading to a high sensitivity to rapid climate change. In response to the 8.2 ka BP event, we find declines in the cover of dominant tree PFTs, but no full transition to another PFT. These different vegetation responses under similar magnitude climate changes indicate the importance of initial climate conditions. Consequently, the resulting vegetation following a climatic perturbation probably depends on the distance between initial climate conditions and climatic thresholds of specific PFT or species (Miller *et al.*, 2008). In addition, Ni *et al.* (2006) suggested that the duration of a climatic perturbation also has the potential to modify the

vegetation response. So, when studying vegetation response to abrupt climate change it is necessary to know both the initial state and the persistence of the climate perturbation.

Uncertainties and outlook

One important source of uncertainty is related to the model–data comparisons and the different scales in these two approaches. In our simulations, vegetation responses are indicated by PFT cover, while in the observations they are represented by percentages of specific pollen taxa (Seppä *et al.*, 2009). Each PFT includes several plant species which are represented by pollen taxa in pollen records. Therefore, the comparisons between simulated PFT cover and percentages of specific pollen taxa are limited to trend comparisons rather than quantitative comparisons. For example, thermophilous deciduous tree pollen taxa often account for only a small proportion, while the associated PFT (TempBS) is the dominant PFT in the model results. This discrepancy could be partially interpreted as reflecting over-representation of *Pinus* in the pollen-based reconstruction due to its long-distance dispersal (Xu *et al.*, 2007). Also, the uncertainties in terms of simulated climate change impact on vegetation simulations and thereby affect model–data comparisons. In particular, the simulated drier conditions could exaggerate the impacts of precipitation on vegetation during the 8.2 ka BP event compared to reconstructed increases in precipitation over Europe. To resolve this issue, more simulations with high-resolution climate models and estimations of the uncertainty range by multiple models simulation need to be made. Additional high-resolution precipitation reconstructions are also called for as a benchmark. In addition, after the 8.2 ka BP event, the simulated climate conditions recover to the 8.5 ka BP level, but in reality due to the different orbital forcing the climate does not return exactly back to the 8.5 ka BP level, leading to uncertainties in the model–data comparison after the 8.2 ka BP event.

On a spatial scale, the smoothed topography in our low-resolution model hardly allows for vegetation changes along altitude gradients, such as the expansions of pine forests captured in pollen at high altitudes over mid-latitudinal Europe (e.g. Tinner and Lotter, 2001) and Southern Europe (e.g. Davis and Stevenson, 2007). By contrast, despite this coarse resolution, our simulation indicates a latitudinal vegetation gradient in the magnitude of responses during the event (Fig. 4), with more pronounced responses to the severe cooling in the north and weaker responses to more moderate cooling in the south. This large-scale gradient is not clear in pollen records, probably because it is masked by many local factors also reflected by pollen records. On a temporal scale, the duration of the 8.2 ka BP event is short compared to the time resolution of most available pollen records, leading to a very limited number of pollen records being suitable for comparisons. Our simulation generally captures the main features of vegetation responses recorded by pollen records, but the possibility of long-lasting impacts of abrupt climate change on vegetation is only indicated by two pollen records (Tinner and Lotter, 2001). We thus need more high-resolution pollen records and simulations studying the long-lasting impacts of abrupt climate changes on vegetation responses.

Conclusions

In this study, we use the 8.5 ka BP and 8.2 ka BP climates simulated by iLOVECLIM to drive a vegetation model (LPJ-GUESS) and investigate the vegetation responses to the 8.2 ka BP event, with a focus on the vegetation changes over Europe and Northern Africa. Based on our analysis, we conclude the following:

1. All dominant PFTs over Europe and North Africa respond to climate change during the 8.2 ka BP event, but the magnitude and timing of their reactions are different. In NWE and NEE, the TempBS fraction is reduced by 17 and 14% within 50 years, respectively, and BoNE experiences a significant expansion (by 12% in NWE and 5% in NEE) after the minimum of TempBS and reaches its peak after 100 years. In WE, TempBS decreases by 7% in about 20 years, while TempBE declines by only 2% in around 60 years, which is slower than for TempBS. In EE, only TempBS decreases by 5% at the beginning of the event. In SE, grasses expand at the expense of TempBE, and tropical trees (only 2%) disappear immediately after cooling begins. In NA, grass cover decreases by 15% in 50 years, followed by a minor expansion (by 2%) of TempBE. After the 8.2 ka BP event, most PFTs return to their pre-perturbed state, except for TempBS which does not recover in NEE, WE and EE. This implies the possibility of different vegetation compositions under similar climate conditions, as a response to an abrupt climate perturbation.
2. When comparing the relative impacts of temperature and precipitation, it is clear that the lower temperature during the 8.2 ka BP event drives the evolution of both BoNE and TempBS in NWE and NEE. In WE and EE, changes in temperature and precipitation alone are not sufficient to drive the decrease in TempBS at the beginning of this event. In SE, temperature is the main driver of the disappearance of tropical trees. In SE, changes in precipitation contribute more to TempBE responses compared with temperature. In NA, the decline of grass cover is caused by changes in both temperature and precipitation, in which the >50% decreases in summer precipitation dominate the grass responses.
3. Our simulation results show a general agreement with pollen records from Europe. The possibility of different vegetation compositions under similar climatic conditions in our simulation is shown in two high-resolution pollen records. These different vegetation compositions could be a long-lasting effect of abrupt climate changes. Moreover, our simulations suggest a latitudinal vegetation gradient, with more pronounced responses to the severe cooling in the north and weaker responses to more moderate cooling in the south. This gradient is not reflected by pollen records.

Acknowledgements. We thank Yurui Zhang for providing the 8.5 ka Bp initial climate conditions. We thank Heikki Seppä for helpful discussion on the comparisons between reconstructed and simulated vegetation. We appreciate the valuable comments and suggestions provided by the three anonymous reviewers which helped improve an earlier version of the manuscript. This work was supported by the China Scholarship Council. P.A.M. acknowledges this as a contribution to the Strategic Research Area MERGE and is grateful for financial support from the Swedish Research Council (VR).

Abbreviations. AMOC, Atlantic Meridional Overturning Circulation; DGVM, dynamic global vegetation model; EE, Eastern Europe; GIS, Greenland Ice Sheet; LGM, Last Glacial Maximum; LIS, Laurentide Ice Sheet; NA, North Africa; PFT, plant functional type; WE, Western Europe.

Supporting information

Additional supporting information may be found in the online version of this article at the publisher's web-site.

Figure S1. DJF surface temperature anomaly between simulated 8.5 ka state (8.5ka_CTRL) and pre-industrial state.
Figure S2. JJA surface temperature anomaly between simulated 8.5 ka state (8.5ka_CTRL) and pre-industrial state.
Figure S3. Annual mean total precipitation anomaly between simulated 8.5 ka state (8.5ka_CTRL) and pre-industrial state.
Figure S4. The maximum annual surface temperature anomaly (50 year mean) during the 8.2 ka BP event (8.2ka_EVENT minus 8.5ka_CTRL). The overlain filled circles show proxy-based reconstructions of surface temperature anomalies associated with the 8.2 ka BP event (Morrill *et al.*, 2013).
Figure S5. Temporal evolution of annual mean temperature anomalies (the left side) and percentage of soil moisture anomalies (the right side) between 8.2ka_EVENT-LPJ and 8.5ka_CTRL-LPJ over (a) NWE, (b) NEE, (c) WE, (d) EE, (e) SE and (f) Northern Africa (NA). The vertical grey bar indicates the start of the climatic 8.2 ka BP event perturbation.
Figure S6. The simulated seasonal temperature anomaly (°C), percentage of precipitation anomaly (%) and soil moisture anomaly (mm) of the 8.2 ka event (8.2ka_EVENT minus 8.5ka_CTRL).
Table. S1 Sites information about pollen records over Europe in Figure 2.
Table. S2 The comparison between modelled 50-year mean surface temperature in 8.2ka_EVENT and it recorded by quantitative temperature proxies (Morrill et al., 2013).

References

Alley R, Agustsdottir A. 2005. The 8k event: cause and consequences of a major Holocene abrupt climate change. *Quaternary Science Reviews* **24**: 1123–1149, https://doi.org/10.1016/j.quascirev.2004.12.004

Andersen T, Carstensen J, Hernández-García E, *et al.* 2009. Ecological thresholds and regime shifts: approaches to identification. *Trends in Ecology and Evolution* **24**: 49–57, https://doi.org/10.1016/j.tree.2008.07.014

Berger A. 1978. Long-term variations of daily insolation and Quaternary climatic changes. *Journal of the Atmospheric Sciences* **35**: 2362–2367, https://doi.org/10.1175/1520-0469(1978)035<2362:LTVODI>2.0.CO;2

Bozbiyik A, Steinacher M, Joos F, *et al.* 2011. Fingerprints of changes in the terrestrial carbon cycle in response to large reorganizations in ocean circulation. *Climate of the Past* **7**: 319–338, https://doi.org/10.5194/cp-7-319-2011

Brovkin V, Ganopolski A, Svirezhev Y. 1997. A continuous climate–vegetation classification for use in climate-biosphere studies. *Ecological Modelling* **101**: 251–261, https://doi.org/10.1016/S0304-3800(97)00049-5

Chervin RM, Schenider SH. 1976. On determining the statistical significance of climate experiments with general circulation models. *Journal of the Atmospheric Sciences* **33**: 405–412, https://doi.org/10.1175/1520-0469(1976)033<0405:ODTSSO>2.0.CO;2

Clarke GKC, Leverington DW, Teller JT, et al. 2004. Paleohydraulics of the last outburst flood from glacial Lake Agassiz and the 8200 BP cold event. *Quaternary Science Reviews* **23**(3-4): 389–407, https://doi.org/10.1016/j.quascirev.2003.06.004

Daley TJ, Thomas ER, Holmes JA, *et al.* 2011. The 8200yr BP cold event in stable isotope records from the North Atlantic region. *Global and Planetary Change* **79**: 288–302, https://doi.org/10.1016/j.gloplacha.2011.03.006

Davis B, Stevenson A. 2007. The 8.2ka event and early–mid Holocene forests, fires and flooding in the Central Ebro Desert, NE Spain. *Quaternary Science Reviews* **26**: 1695–1712, https://doi.org/10.1016/j.quascirev.2007.04.007

Feurdean A, Bennike O. 2004. Late Quaternary palaeoecological and palaeoclimatological reconstruction in the Gutaiului Mountains, northwest Romania. *Journal of Quaternary Science* **19**: 809–827, https://doi.org/10.1002/jqs.872

Feurdean A, Klotz S, Mosbrugger V, *et al.* 2008. Pollen-based quantitative reconstructions of Holocene climate variability in NW Romania. *Palaeogeography, Palaeoclimatology, Palaeoecology* **260**: 494–504, https://doi.org/10.1016/j.palaeo.2007.12.014

Fiłoc M, Kupryjanowicz M, Szeroczyńska K, *et al.* 2017. Environmental changes related to the 8.2 ka event and other climate fluctuations during the Middle Holocene: evidence from two dystrophic lakes in NE Poland. *The Holocene* **27**: 1550–1566, https://doi.org/10.1177/0959683617702233

Ghilardi B, O'Connell M. 2013. Early Holocene vegetation and climate dynamics with particular reference to the 8.2 ka event: pollen and macrofossil evidence from a small lake in western Ireland. *Vegetation History and Archaeobotany* **22**: 99–114, https://doi.org/10.1007/s00334-012-0367-x

Goosse H, Brovkin V, Fichefet T, *et al.* 2010. Description of the Earth system model of intermediate complexity LOVECLIM version 1.2. *Geoscientific Model Development* **3**: 603–633, https://doi.org/10.5194/gmd-3-603-2010

Haxeltine A, Prentice IC. 1996. BIOME3: an equilibrium terrestrial biosphere model based on ecophysiological constraints, resource availability, and competition among plant functional types. *Global Biogeochemical Cycles* **10**: 693–709, https://doi.org/10.1029/96GB02344

Head K, Turney CSM, Pilcher JR, *et al.* 2007. Problems with identifying the '8200-year cold event' in terrestrial records of the Atlantic seaboard: a case study from Dooagh, Achill Island, Ireland. *Journal of Quaternary Science* **22**: 65–75, https://doi.org/10.1002/jqs.1006

Hede MU, Rasmussen P, Noe-Nygaard N, et al. 2010. Multiproxy evidence for terrestrial and aquatic ecosystem responses during the 8.2 ka cold event as recorded at HøjbySø, Denmark. *Quaternary Research* **73**(03): 485–496.

Joly C, Visset L. 2009. Evolution of vegetation landscapes since the Late Mesolithic on the French west Atlantic coast. *Review of Palaeobotany and Palynology* **154**: 124–179, https://doi.org/10.1016/j.revpalbo.2008.12.011

Kobashi T, Severinghaus JP, Brook EJ, *et al.* 2007. Precise timing and characterization of abrupt climate change 8200 years ago from air trapped in polar ice. *Quaternary Science Reviews* **26**: 1212–1222, https://doi.org/10.1016/j.quascirev.2007.01.009

Köhler P, Joos F, Gerber S, *et al.* 2005. Simulated changes in vegetation distribution, land carbon storage, and atmospheric CO_2 in response to a collapse of the North Atlantic thermohaline circulation. *Climate Dynamics* **25**: 689–708, https://doi.org/10.1007/s00382-005-0058-8

Kotthoff U, Pross J, Müller UC, *et al.* 2008. Climate dynamics in the borderlands of the Aegean Sea during formation of sapropel S1 deduced from a marine pollen record. *Quaternary Science Reviews* **27**: 832–845, https://doi.org/10.1016/j.quascirev.2007.12.001

Lees AK, Wattier R, Shaw DS, *et al.* 2006. Novel microsatellite markers for the analysis of Phytophthorainfestans populations. *Plant Pathology* **55**: 311–319, https://doi.org/10.1111/j.1365-3059.2006.01359.x

Loulergue L, Schilt A, Spahni R, *et al.* 2008. Orbital and millennial-scale features of atmospheric CH_4 over the past 800,000 years. *Nature* **453**: 383–386, https://doi.org/10.1038/nature06950

Lu Z, Miller PA, Zhang Q, *et al.* 2018. Dynamic vegetation simulations of the mid-Holocene Green Sahara. *Geophysical Research Letters* **45**: 8294–8303, https://doi.org/10.1029/2018GL079195

Matero ISO, Gregoire LJ, Ivanovic RF, *et al.* 2017. The 8.2 ka cooling event caused by Laurentide ice saddle collapse. *Earth and Planetary Science Letters* **473**: 205–214, https://doi.org/10.1016/j.epsl.2017.06.011

Meissner KJ, Clark PU. 2006. Impact of floods versus routing events on the thermohaline circulation. *Geophysical Research Letters* **33**: L15704, https://doi.org/10.1029/2006GL026705

Menviel L, Timmermann A, Mouchet A, *et al.* 2008. Meridional reorganizations of marine and terrestrial productivity during Heinrich events. *Paleoceanography* **23**: PA1203, https://doi.org/10.1029/2007PA001445

Miller PA, Giesecke T, Hickler T, *et al.* 2008. Exploring climatic and biotic controls on Holocene vegetation change in Fennoscandia. *Journal of Ecology* **96**: 247–259, https://doi.org/10.1111/j.1365-2745.2007.01342.x

Morrill C, Anderson DM, Bauer BA, *et al.* 2013. Proxy benchmarks for intercomparison of 8.2 ka simulations. *Climate of the Past* **9**: 423–432, https://doi.org/10.5194/cp-9-423-2013

Morrill C, Ward EM, Wagner AJ, *et al.* 2014. Large sensitivity to freshwater forcing location in 8.2 ka simulations. *Paleoceanography* **29**: 930–945, https://doi.org/10.1002/2014PA002669

Nesje A, Bjune AE, Bakke J, *et al.* 2006. Holocene palaeoclimate reconstructions at Vanndalsvatnet, western Norway, with particular reference to the 8200 cal. yr BP event. *The Holocene* **16**: 717–729, https://doi.org/10.1191/0959683606hl954rp

Ni J, Harrison SP, Colin Prentice IC, *et al.* 2006. Impact of climate variability on present and Holocene vegetation: a model-based study. *Ecological Modelling* **191**: 469–486, https://doi.org/10.1016/j.ecolmodel.2005.05.019

Novenko EY, Olchev AV. 2015. Early Holocene vegetation and climate dynamics in the central part of the East European Plain (Russia). *Quaternary International* **388**: 12–22, https://doi.org/10.1016/j.quaint.2015.01.027

Opsteegh JD, Haarsma RJ, Selten FM, et al. 1998. ECBILT: a dynamic alternative to mixed boundary conditions in ocean models. *Tellus Series A* **50**: 348–367.

Pál I, Magyari EK, Braun M, *et al.* 2016. Small-scale moisture availability increase during the 8.2 ka climatic event inferred from biotic proxy records in the South Carpathians (SE. *Romania). The Holocene* **26**: 1382–1396, https://doi.org/10.1177/0959683616640039

Peltier WR. 2004. Global glacial isostasy and the surface of the Ice-Age Earth: the ICE-5G (VM2) model and Grace. *Annual Review of Earth and Planetary Sciences* **32**: 111–149, https://doi.org/10.1146/annurev.earth.32.082503.144359

Roche DM, Dumas C, Bügelmayer M, *et al.* 2014. Adding a dynamical cryosphere to iLOVECLIM (version 1.0): coupling with the GRISLI ice-sheet model. *Geoscientific Model. Development* **7**: 1377–1394, https://doi.org/10.5194/gmd-7-1377-2014

Rohling EJ, Pälike H. 2005. Centennial-scale climate cooling with a sudden cold event around 8,200 years ago. *Nature* **434**: 975–979, https://doi.org/10.1038/nature03421

Rosén P, Segerström U, Eriksson L, *et al.* 2001. Holocene climatic change reconstructed from diatoms, chironomids, pollen and near-infrared spectroscopy at an alpine lake (Sjuodjijaure) in northern Sweden. *The Holocene* **11**: 551–562, https://doi.org/10.1191/095968301680223503

Sarmaja-Korjonen K, Seppä H. 2007. Abrupt and consistent responses of aquatic and terrestrial ecosystems to the 8200 cal. yr cold event: a lacustrine record from Lake Arapisto, Finland. *The Holocene* **17**: 457–467, https://doi.org/10.1177/0959683607077020

Schilt A, Baumgartner M, Schwander J, *et al.* 2010. Atmospheric nitrous oxide during the last 140,000 years. *Earth and Planetary Science Letters* **300**: 33–43, https://doi.org/10.1016/j.epsl.2010.09.027

Scholze M, Knorr W, Heimann M. 2003. Modelling terrestrial vegetation dynamics and carbon cycling for an abrupt climatic change event. *The Holocene* **13**: 327–333, https://doi.org/10.1191/0959683603hl625rp

Seppä H, Alenius T, Muukkonen P, *et al.* 2009. Calibrated pollen accumulation rates as a basis for quantitative tree biomass reconstructions. *The Holocene* **19**: 209–220, https://doi.org/10.1177/0959683608100565

Seppä H, Birks HJB, Giesecke T, *et al.* 2007. Spatial structure of the 8200 cal yr BP event in northern Europe. *Climate of the Past* **3**: 225–236, https://doi.org/10.5194/cp-3-225-2007

Seppä H, Poska A. 2004. Holocene annual mean temperature changes in Estonia and their relationship to solar insolation and atmospheric circulation patterns. *Quaternary Research* **61**: 22–31, https://doi.org/10.1016/j.yqres.2003.08.005

Seppä H, Schurgers G, Miller PA, *et al.* 2015. Trees tracking a warmer climate: the Holocene range shift of hazel (*Corylus avellana*) in northern. *Europe. The Holocene* **25**: 53–63, https://doi.org/10.1177/0959683614556377

Sitch S, Smith B, Prentice IC, *et al.* 2003. Evaluation of ecosystem dynamics, plant geography and terrestrial carbon cycling in the LPJ dynamic global vegetation model. *Global Change Biology* **9**: 161–185, https://doi.org/10.1046/j.1365-2486.2003.00569.x

Smith B, Prentice IC, Sykes MT. 2001. Representation of vegetation dynamics in the modelling of terrestrial ecosystems: comparing two contrasting approaches within European climate space. *Global Ecology and Biogeography* **10**: 621–637, https://doi.org/10.1046/j.1466-822X.2001.00256.x

Smith B, Wårlind D, Arneth A, *et al.* 2014. Implications of incorporating N cycling and N limitations on primary production in an individual-based dynamic vegetation model. *Biogeosciences* **11**: 2027–2054, https://doi.org/10.5194/bg-11-2027-2014

Snowball I, Zillén L, Gaillard M-J. 2002. Rapid early-Holocene environmental changes in northern Sweden based on studies of two varved lake-sediment sequences. *The Holocene* **12**: 7–16, https://doi.org/10.1191/0959683602hl515rp

Sykes MT, Prentice IC, Cramer W. 1996. A bioclimatic model for the potential distributions of North European tree species under present and future climates. *Journal of Biogeography* **23**: 203–233.

Thomas ER, Wolff EW, Mulvaney R, *et al.* 2007. The 8.2ka event from Greenland ice cores. *Quaternary Science Reviews* **26**: 70–81, https://doi.org/10.1016/j.quascirev.2006.07.017

Tinner W, Lotter AF. 2001. Central European vegetation response to abrupt climate change at 8.2 ka. *Geology* **29**: 551–554, https://doi.org/10.1130/0091-7613(2001)029<0551:CEVRTA>2.0.CO;2

Torbenson MCA, Plunkett G, Brown DM, *et al.* 2015. Asynchrony in key Holocene chronologies: evidence from Irish bog pines. *Geology* **43**: 799–802, https://doi.org/10.1130/G36914.1

Törnqvist TE, Bick SJ, González JL, *et al.* 2004. Tracking the sea-level signature of the 8.2 ka cooling event: new constraints from the Mississippi Delta. *Geophysical Research Letters* **31**: L23309, https://doi.org/10.1029/2004GL021429

Veski S, Seppä H, Ojala AEK. 2004. Cold event at 8200 yr B.P. recorded in annually laminated lake sediments in eastern Europe. *Geology* **32**: 681, https://doi.org/10.1130/G20683.1

Wagner AJ, Morrill C, Otto-Bliesner BL, *et al.* 2013. Model support for forcing of the 8.2 ka event by meltwater from the Hudson Bay ice dome. *Climate Dynamics* **41**: 2855–2873, https://doi.org/10.1007/s00382-013-1706-z

Wiersma AP, Renssen H. 2006. Model–data comparison for the 8.2kaBP event: confirmation of a forcing mechanism by catastrophic drainage of Laurentide Lakes. *Quaternary Science Reviews* **25**: 63–88, https://doi.org/10.1016/j.quascirev.2005.07.009

Wiersma AP, Roche DM, Renssen H. 2011. Fingerprinting the 8.2 ka event climate response in a coupled climate model. *Journal of Quaternary Science* **26**: 118–127, https://doi.org/10.1002/jqs.1439

Woillez M-N, Kageyama M, Combourieu-Nebout N, *et al.* 2013. Simulating the vegetation response in Western Europe to abrupt climate changes under glacial background conditions. *Biogeosciences* **10**: 1561–1582, https://doi.org/10.5194/bg-10-1561-2013

Xu Q, Li Y, Yang X, *et al.* 2007. Quantitative relationship between pollen and vegetation in northern China. *Science in China Series D* **50**: 582–599, https://doi.org/10.1007/s11430-007-2044-y

Zhang Y, Renssen H, Seppä H. 2016. Effects of melting ice sheets and orbital forcing on the early Holocene warming in the extratropical Northern Hemisphere. *Climate of the Past* **12**: 1119–1135, https://doi.org/10.5194/cp-12-1119-2016

